2010

The lack of intense Lyman~alpha in ultradeep spectra of z=7 candidates in GOODS-S: imprint of reionization?

A. Fontana
E. Vanzella
L. Pentericci
M. Castellano
Mauro Giavalisco, *University of Massachusetts - Amherst*, et al.

Draft version October 15, 2010
Preprint typeset using LaTeX style emulateapj v. 11/10/09

THE LACK OF INTENSE LYMAN α IN ULTRADEEP SPECTRA OF $Z = 7$ CANDIDATES IN GOODS-S: IMPRINT OF REIONIZATION?

A. Fontana[1], E. Vanzella [2] L. Pentericci, [1] M. Castellano [1] M. Giavalisco [3] A. Grazian [1] K. Boutsia [1] S. Cristiani [2] M. Dickinson[4] E. Giallongo [1] M. Maiolino, [1] A. Moorwood [5] P. Santini [1]
INAF Osservatorio Astronomico di Roma, Via Frascati 33,00040 Monteporzio (RM), Italy
INAF Osservatorio Astronomico di Trieste, Via G.B.Tiepolo 11, 34131 Trieste, Italy
Department of Astronomy, University of Massachusetts, 710 North Pleasant Street, Amherst, MA 01003
National Optical Astronomy Observatory, PO Box 26732, Tucson, AZ 85726, USA and
European Southern Observatory, Karl-Schwarzschild Strasse, 85748 Garching bei Munchen, Germany
Draft version October 15, 2010

ABSTRACT

We present ultradeep optical spectroscopy obtained with FORS2 on VLT of seven Lyman–break galaxy (LBG) candidates at $z > 6.5$ selected in the GOODS–S field from Hawk–I/VLT and WFC3/HST imaging. For one galaxy we detect a low significance emission line ($S/N \leq 7$), located at $\lambda = 9691.5 \pm 0.5$ Å and with flux 3.4×10^{-18}erg cm^{-2}s^{-1}. If identified as Lyα, it places the LBG at redshift $z = 6.972 \pm 0.002$, with a rest–frame equivalent width $EW_{rf} = 13$Å. Using Monte Carlo simulations and conservative EW distribution functions at $2 < z < 6$, we estimate that the probability of observing no galaxies in our data with $S/N > 10$ is $\simeq 2\%$, and that of observing only one galaxy out of seven with $S/N = 5$ is $\simeq 4\%$, but these can be as small as $\sim 10^{-3}$, depending on the details of the EW distribution. We conclude that either a significant fraction of the candidates is not at high redshift or that some physical mechanism quenches the Lyα emission emerging from the galaxies at $z > 6.5$, abruptly reversing the trend of the increasing fraction of strong emitters with increasing redshift observed up to $z \sim 6.5$. We discuss the possibility that an increasingly neutral intergalactic medium is responsible for such quenching.

Subject headings: galaxies: distances and redshifts - galaxies: high-redshift - galaxies: formation

1. INTRODUCTION

During the past year, a suite of new near–infrared (NIR) surveys has extended the search for star–forming galaxies to redshift $6.5 \leq z \leq 10$ using the well–proven Lyman–break technique (Giavalisco 2002, and references therein). With respect to lower redshift, the number density of UV–selected galaxies decreases (e.g., Ouchi et al. 2009; McLure et al. 2010; Castellano et al. 2010; Bouwens et al. 2010a; Wilkins et al. 2010b), their UV continuum becomes bluer implying either reduced dust obscuration or poorer metal enrichment or both (e.g., Finkelstein et al. 2009; Bouwens et al. 2010b; Schaerer & de Barros 2010), and their stellar masses are, on average, smaller than those of their lower redshift counterparts (e.g., Labbé et al. 2010). Unfortunately, these results are based on color-selected samples with no spectroscopic validation. At the time of writing, spectroscopic detections of only a few individual objects have been obtained at $z > 6.6$ (Iye et al. 2006; Greiner et al. 2009; Salvaterra et al. 2009; Tanvir et al. 2009).

The lack of knowledge of the true redshifts of the current $z \sim 7$ candidates places significant limitations on our ability to robustly measure the properties of the galaxies at this critical cosmic epoch. For example, the fraction of interlopers and the redshift distribution of the sample galaxies are necessary to robustly measure the UV luminosity function (e.g., Reddy & Steidel 2009). Currently, the former remains unknown, and the latter is estimated with Monte Carlo simulations under various assumptions for the intrinsic distributions of UV spectral energy distribution (SED), surface brightness and morphology, with the result that the measure of the luminosity function remains subject to uncontrolled systematic errors.

In practice, given the marked decrease in sensitivity of current spectroscopic observations at increasing redshift, the spectral confirmation of galaxies at $z > 5$ relies heavily on their Lyα emission line, (Stark et al. 2010; Vanzella et al. 2009, S10 and V09 in the following). Indeed, redshifts derived without Lyα typically have lower confidence, although their number may be comparable (Douglas et al. 2010, D10 in the following). The line in itself is an important diagnostic of physical processes at work in the galaxies (e.g., Giavalisco et al. 1996; Pentericci et al. 2010; Shapley et al. 2003), since its strength and velocity profile depend on the instantaneous star-formation rate, dust content, metallicity, kinematics and geometry of the interstellar medium. Particularly relevant here is the evidence that the fraction of Lyα emitters in UV–selected samples increases with redshift (V09,S10 Reddy & Steidel 2009; Stanway et al. 2007, S07 in the following) and that the fraction of galaxies with a large Lyα equivalent width (EW) is substantially larger at fainter UV luminosities.

Finally, the very visibility of the Lyα line during the ending phases of the cosmic re–ionization is subject to the damping effect of an increasing neutral intergalactic medium (IGM) (e.g., Zheng et al. 2010; Dayal et al. 2010), expected to attenuate most of its luminosity and make the earliest galaxies consequently more difficult to identify. Hence, the line profile and the evolution of its EW are sensitive diagnostics of the ionization state of

adriano.fontana@oa-roma.inaf.it

the high redshift IGM.

To address these issues we have started a campaign of spectroscopic follow-up of $z \simeq 7$ "Z–dropout" candidates, selected from high–quality imaging surveys obtained with VLT/Hawk-I and *HST*/WFC3. In this paper we present the first results from a sample selected in the GOODS–S field (Castellano et al. 2010, C10 in the following). All magnitudes are in the AB system, and we adopt $H_0 = 70$ km/s/Mpc, $\Omega_M = 0.3$ and $\Omega_\Lambda = 0.7$.

2. TARGETS AND SPECTROSCOPIC DATA

This initial spectroscopic sample includes relatively bright Lyman break galaxy (LBG) candidates at $z > 6.5$ (listed in Table 1), five from the Hawk–I images (4 from C10 and 1 from Hickey et al. (2010)) and two from WFC3 (Oesch et al. 2010; Wilkins et al. 2010a), spanning the magnitude range $Y \simeq 25.5-27.5$. We filled empty slitlets in the multi-object slit masks with other candidates of lower quality and/or at lower redshift, including a candidate brown dwarf (Mannucci et al. (2007), C10) and i–dropouts from the GOODS survey not observed by V09.

2.1. *Observations*

Observations were taken in service mode with the FORS2 spectrograph on the ESO Very Large Telescope, between 12 November 2009 and 14 January 2010. We used the 600Z holographic grating, that provides the highest sensitivity in the range $8000 - 10000$Å with a spectral resolution $R \simeq 1390$ and a sampling of 1.6Å per pixel for a 1" slit. The data presented here come from the coaddition of 75 spectra of 842 seconds of integration each, on a single mask, for a grand total of 63150 s (17.5 hr), with median seeing around 0.8". Each slitlet was 1" wide and 14" long, to maximize the number of slits available while allowing a careful sky subtraction. All our high priority targets were placed at the center of the slits, and spectra were taken in series of three different positions, offset by ±2" in the direction perpendicular to the dispersion.

Since our objects are extremely faint, the slit centering was based on the astrometry solution obtained from the Hawk–I images, which is which is well aligned to the ACS one. We have directly verified this by placing a few bright objects from the ACS catalogs in small slits, and ensuring that they were correctly aligned during the observations. It is also reassuring to note that three faint i-dropouts selected from the ACS catalog which were placed in slitlets using the same astrometry, have a clear Lyα detection at $z \simeq 5.94$ (full details will be given in a future paper).

Data reduction was performed using an optimized version of the recipes adopted in V09 and previous papers. After standard flat-fielding and wavelength calibration, we subtracted the sky emission lines with two different procedures. In the first case (Polyn in the following) we fit polynomials of order n (from 1 to 5) to the sky intensity at each pixel position. This procedure in principle ensures the highest S/N, but is sensitive to systematics induced by defects in the detector or in the slit manufacturing. A safer but somewhat noisier approach (ABBA in the following) is to subtract the sky background between two consecutive exposures, exploiting the fact that the target spectrum is offset due to dithering. We found the spectra obtained with the two techniques entirely consistent. Finally, spectra were flux-calibrated using the observations of spectrophotometric standards. Slit losses are small, given the extremely compact size of the targets and we neglect them in the subsequent analysis.

The r.m.s. of the resulting spectra, which will be used later to determine the probability of our results with a Monte Carlo simulation, has been estimated "by first principles", i.e., computing the absolute r.m.s. of each frame from its raw counts c as $\sqrt{(c/g)}$ (where g is the e^--ADU conversion factor) and propagating it through all the reduction steps. It turned to be in excellent agreement with the observed r.m.s. in the region between 8150 and 8250Å that is devoid of sky lines and with the predicted efficiencies estimated by the ESO exposure time calculator. The resulting 1σ limiting flux density is shown in the lower panel of Fig.1.

To obtain the corresponding limit on the detectable EW for a Lyα line, we have computed three differ-

TABLE 1
z-DROP TARGETS IN GOODS-S

ID	R.A. (deg)	DEC. (deg)	Y	Z-Y	$M_{UV}^{(a)}$
G2_1408[b]	53.177382	-27.782416	26.37	>2.1	-20.49
G2_2370[b]	53.094421	-27.716847	25.56	1.68	-21.27
G2_4034[b]	53.150019	-27.744914	26.35	>2.1	-20.50
G2_6173[b]	53.123074	-27.701256	26.53	>1.9	-20.33
H_9136[c]	53.072574	-27.728610	25.90	1.29	-20.94
W_6[d]	53.100392	-27.703847	26.93	1.17	-20.38
O_5[e]	53.177376	-27.7920551	27.52	1.61	-19.67

a - Computed at $z = 6.8$
b - Castellano et al. (2010), Y_{OPEN} Hawk-I
c - Hickey et al. (2010), Y_{OPEN} Hawk-I
d - Wilkins et al. (2010a), Y_{098} WFC3 - ERS
e - Oesch et al. (2010), Y_{105} WFC3 - HUDF

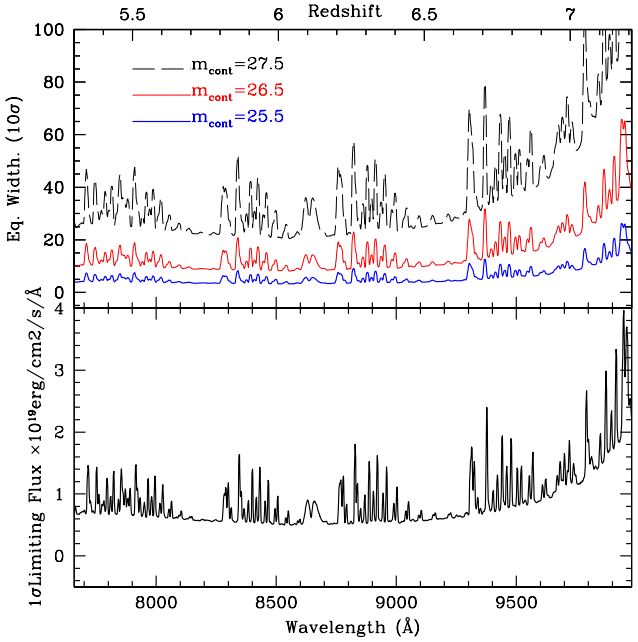

FIG. 1.— *Lower:* Limiting flux density (at 1σ level) resulting from our observations. *Upper:* Corresponding 10σ limit on the rest-frame equivalent width of a Lyα emission line as a function of redshift. Colors and line widths correspond to different observed magnitudes in the Y band, as shown in the legend.

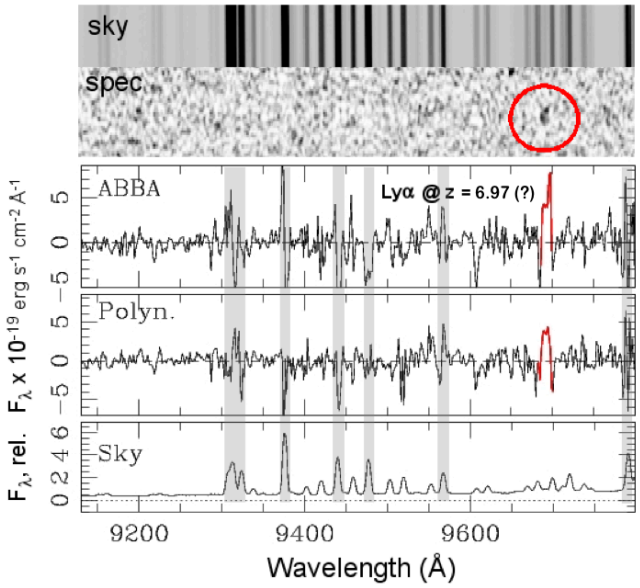

FIG. 2.— Spectrum of the candidate G2_1408, showing a tentative emission line at 9691.5Å. The two upper panels show the 2–D spectrum of the sky emission and of the sky-subtracted object, as indicated. The x-axis is in wavelength, in the same range of the three spectra below. The 2-D spectrum of the galaxy has been divided by the r.m.s. to remove obvious spikes due to bright sky lines, and slightly filtered with an adaptive mesh. The three 1-D spectra in the lower part show the extracted spectrum (over 4 pixels) with the two different techniques for sky subtraction, and the sky emission at the same wavelengths (see legend). In these panels the spectra have not been divided by the r.m.s., nor filtered.

ent cases, assuming continuum magnitudes of $m = 25.5, 26.5, 27.5$, to span the luminosity range of our targets. For the computation we assume that the flux profile is a Gaussian with FWHM= 10Å. The resulting limiting EW is shown in the upper panel of Fig.1, computed at the 10σ level. We could detect weak ($EW \simeq 5$Å) Lyα lines in our brightest galaxies, and even for the faintest ones we are able to reach $EW \simeq 50$Å over a significant fraction of the redshift interval. This range of sensitivity is similar to that of $z \simeq 5-6$ surveys (S07, V09, D10, S10).

2.2. *Results*

We detect only one weak emission line, centered at 9691.5 ± 0.5Å in the spectrum of the object G2_1408. This galaxy is the brightest candidate identified in the Hubble Ultradeep Field (HUDF) area, and one of the brightest in C10. It was first detected by Bouwens et al. (2004) in the NICMOS HUDF data, and subsequently identified also by C10 and in the HUDF WFC3 data (Bouwens et al. 2010a; Oesch et al. 2010; McLure et al. 2010; Bunker et al. 2009). From the clear elongation observed in the WFC3 images, one can exclude the possibility that it is a brown dwarf. The 2-D and 1-D spectra of G2_1408 are shown in Fig.2 The spectral feature is extended over 4 pixels in the spatial direction, consistent with the average seeing. The FWHM is $\simeq$ 10Å, significantly larger than any feature due to noise. The weak emission line has a total observed flux of 3.4×10^{-18}erg cm^{-2}s^{-1}. The formal S/N is 7, but this estimate does not include systematic errors, and should be considered as an upper limit. We made extensive tests to verify the reliability of this detection. We verified that the feature is present both in the Polyn and in the ABBA reductions, as shown in Fig.2. We then inspected all the 75 individual spectra to ensure that the feature is not due to an artifact, and that it is still detected when we separately summed the data in two halves. Because of the large color break ($z - Y > 2.1$) measured in the HUDF data and the non–detection in the BVI bands, an identification of this line with a lower redshift [OII] or Hα would imply a very peculiar SED, unlike that of currently known galaxies. This cannot be excluded a priori.

We note that there is no evidence of the asymmetry that is expected (but not required, see discussion below) for a $z \simeq 7$ galaxy, although the S/N is too poor to reach any firm conclusion about this.

Based on these tests, we conclude that the feature is likely real and due to Lyα emission from a $z = 6.972$ galaxy ($z = 6.970$ if computed at the blue edge of the line), although this should be validated by independent and possibly deeper observations. No continuum is detected in the spectrum: if we estimate it from the Hawk–I Y-band magnitude (Table 1), the line flux translates into an observed EW of 103Å, corresponding to 13Å if placed at $z = 6.972$.

We do not identify any other emission lines from objects in our sample. We only detect a faint continuum from two objects, namely G2_2370 (the brightest in our sample) and the brown dwarf candidate of Mannucci et al. (2007). In both cases, the continuum is consistent with the broad–band magnitudes but the low S/N prevents us from deriving any robust information about their spectral type or redshift.

3. THE EXPECTED NUMBER OF Lyα DETECTIONS

The key result of our observations is the lack of prominent Lyα emission lines in our sample, which may imply a rapid evolution in the physical properties of $z > 6$ galaxies and/or in the surrounding IGM. To quantify this issue, we have carried out the following Monte Carlo simulations under the assumptions that *a)* all our 7 candidates are indeed $z \simeq 7$ galaxies; and *b)* the distribution of the Lyα intensity in galaxies as a function of their rest–frame continuum magnitude M_{UV} does not change significantly from $z = 4-6$ to $z = 7$.

For the redshift distribution expected for our sample we use the result by C10 (see their Fig 7), which has a broad maximum from $z = 6.4$ to $z = 7.1$ and tails that extend to $z = 6$ and $z = 7.5$. The distribution of the Lyα intensity in galaxies at $z = 3-6$ has been investigated in a number of studies (S07, V09, S10, D10), showing that the intensity of Lyα is anti–correlated with rest–frame UV luminosity. No measure of the dependence of the EW distribution as a function of M_{UV} has been obtained, however. We model the EW distribution assuming that at EW$>$ 0 it is represented by a Gaussian centered on EW=0 with an additional constant tail up to 150Å, and at EW$<$ 0 by a constant level down to some EW$_{min}$ value, and null below. We take the width of the Gaussian and the two tails to reproduce the results of V09 and S10 at different rest–frame magnitudes. Specifically, we derive from the bright galaxies in V09 a standard deviation for the Gaussian of 10Å, and assume that it is constant at all magnitudes. We then divide our sample in two luminosity bins ($-20.5 < M_{UV}$ and

$-20.5 < M_{UV} < -19.5$) and adjust the two tails in order to reproduce the fraction of galaxies with $EW > 50$Å given by S10 and the fraction of galaxies with EW > 5 and EW> 20 Å (for the two bins, respectively), as given by the V09 data. The resulting distributions are shown in Figure 3 for the two magnitude bins, and are reasonably similar in shape to the EW distribution at $z \simeq 5-6$ (S07), and show a moderate evolution from the $z \simeq 3-5$ (Shapley et al. 2003, D10) one.

We then compute the probability of detecting N Lyα lines at a given S/N in our sample of 7 objects. For each object we randomly extract a redshift from the C10 distribution, we compute the corresponding M_{UV} from the observed Y band magnitude (taking into account the IGM absorption at that redshift), and we then randomly extract an EW from the corresponding distribution. If the EW is larger than the minimum detectable EW at the corresponding wavelength (Fig.1) for a given S/N we conclude that the object would be detected. We assume FWHM=10Å for the line, as found at $z = 6.9$ by Iye et al. (2006) (see also Fig.1). Clearly, intrinsically broader lines would be harder to detect. We perform this exercise 10^5 times over the whole sample, requiring S/N> 10 for the detection (larger than the S/N of the possible detection in G2_1408), and we finally obtain the probability distribution shown in the lower panel of Fig. 3. Under these assumptions, the probability of detecting no Lyα line in our sample is very small, about 2%, while the typical number of Lyα that we should have detected is between 2 and 4. We also find a low probability (4%) of having 1 detection at S/N> 5, as found in our sample. The same probability adopting the S07 distribution would be much smaller ($\simeq 10^{-3}$), because of the substantial tail of objects with large EW. Even using the Shapley et al. (2003) distribution, which has a lower fraction of high EW objects, the probability is still rather low (9%). We conclude that, with all the obvious caveats due to the small size of our sample and to possible observational mishaps, the lack of prominent Lyα lines in our sample is statistically significant.

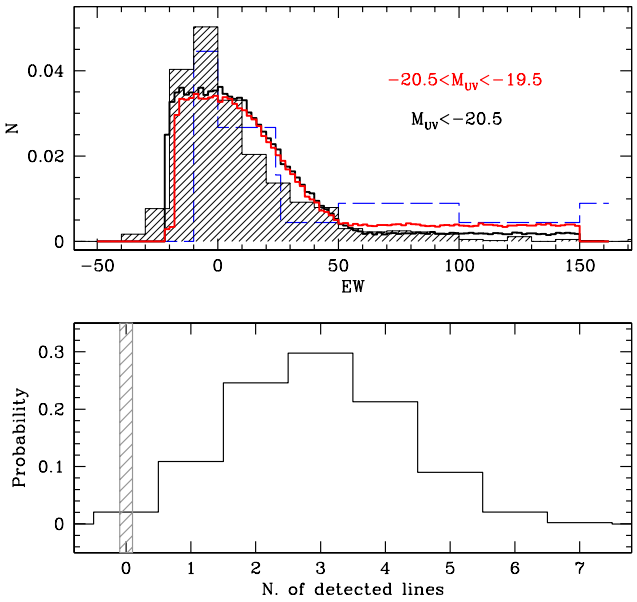

FIG. 3.— Simulations on the expected number of Lyα emitters in our sample. *Upper:* The adopted distribution of rest-frame EW for the two extreme values of rest-frame UV luminosities in our sample (red and black continuous histogram). The shaded histogram shows the Shapley et al. (2003) distribution at $z \simeq 3$ and the blue dashed histogram shows the Stanway et al. (2007) distribution at $z \simeq 4-6$. *Lower:* The resulting probability of detecting N lines with S/N> 10 in our sample, using the simulations described in the text. We observe no Lyα with S/N> 10.

.

4. IMPLICATIONS AND DISCUSSION

On a practical level, our results show how challenging it is to obtain large samples of spectroscopically confirmed galaxies at $z > 6.5$ with current instrumentation, especially if one aims at reaching the level of completeness ($\gg 50\%$) needed to robustly measure the luminosity function. Our observations imply that this goal will have to wait until a future generation of instruments is available, either 8m telescopes equipped with multi-object spectrographs more efficient in the z and Y bands or, more likely, the new generation of telescopes, such as the *James Webb Space Telescope* or 20-40m ground-based facilities. Nonetheless, our analysis appears to show that the failure to detect prominent Lyα in our sample is not only due to the insufficiency of current instrumentation.

One possibility is that a significant fraction of the candidates are lower redshift interlopers. We test this possibility by extrapolating to $z \sim 7$ the observed contamination in spectroscopic samples at $z \sim 4$, 5 and 6 (V09, Table 4 of B, V and i dropouts), which increases with redshift. We assume that amongst our z–band dropout sample the fraction of contaminants could be ∼25%, i.e., 2 out of 7 candidates. This estimate may be pessimistic, given the excellent photometric quality of the Hawk–I and WFC3 data, and the more careful cleaning of lower z interlopers compared to the V09 samples. However, the contaminant population may be changing at higher redshifts, and different and previously unstudied galaxy types may be entering the selection window. Ignoring these uncertainties, we repeated the Monte Carlo simulation for all possible choices of 5 candidates from our 7, finding that the probability of detecting no Lyα line at S/N> 10 is still rather low, being typically 8%, and only in one case reaching 15% (this range depends on which candidates are excluded from the sample).

Another explanation for the paucity of Lyα detections would be physical evolution of either the galaxies or the surrounding IGM. The intrinsic strength of the Lyα emission is expected to increase at higher redshift as galaxies become more metal- and dust-poor. The probability that these photons escape the galaxy and its surroundings, however, depends on a series of complex (and not fully characterized) phenomena in the IGM surrounding the galaxies (Zheng et al. 2010, and references therein), including the relative geometry and dynamics of gas and dust, e.g., backward scattering from wind–driven outflowing shells (which can even boost the strength of the lines), or absorption by the damping wings of in-falling IGM along the line of sight. The presence of HI in proximity to the source can result in an absorption of the intrinsic Lyα by one order of magnitude or more (Zheng et al. 2010), along with a broadening and redshifting of the emerging line profile. Thus, one explanation for the

lack of Lyα detections in our sample is a significant increase in the HI fraction of the IGM, χ_{HI}, at $z \sim 7$, leading to a stronger absorption of the Lyα flux. A similar effect could explain the observed decrease in the number of Lyα emitters at $z \simeq 7$ (Ota et al. 2010, Clément et al., in prep.), but results from these surveys are still contradictory (Ouchi et al. 2010; Hu et al. 2010). Detailed simulations (Dayal et al. 2010) show that the IGM absorption increases dramatically when the Universe is not fully ionized, leading to a significant absorption of the emerging Lyα. The timescale of this effect around star–forming galaxies is of the order of 100 Myr (Dayal et al. 2010), shorter than the interval of cosmic time between $z \simeq 6.$ and $z \simeq 7$. An additional prediction is that the asymmetry in the line profile is smoothed by the velocity structure of the infalling IGM (Dayal et al. 2008). Unfortunately, the modest S/N in our only detection is too low to address this effect quantitatively.

In conclusion, this work shows that the spectroscopic confirmation of $z \simeq 7$ galaxy candidates is a challenging effort. However, these difficulties may not be only due to our current technological limits, but may also reflect the long–sought first evidence of the reionization process in the early Universe. Future surveys will definitely solve this fascinating puzzle.

Observations were carried out using the Very Large Telescope at the ESO Paranal Observatory under Programme IDs 084.A-095, 181.A-0717. We thank an anonymous referee for precious comments. We are grateful to P. Møller and the whole ESO staff for their assistance during the execution of service observations. We acknowledge partial financial support by ASI.

REFERENCES

Bouwens, R. J., Illingworth, G. D., Oesch, P. A., et al. 2010a, ApJ, 709, L133
Bouwens, R. J., Illingworth, G. D., Oesch, P. A., et al. 2010b, ApJ, 708, L69
Bouwens, R. J., Thompson, R. I., Illingworth, G. D., et al. 2004, ApJ, 616, L79
Bunker, A., Wilkins, S., Ellis, R., et al. 2009, ArXiv e-prints
Castellano, M., Fontana, A., Boutsia, K., et al. 2010, A&A, 511, A20+ (C10)
Dayal, P., Ferrara, A., & Gallerani, S. 2008, MNRAS, 389, 1683
Dayal, P., Maselli, A., & Ferrara, A. 2010, ArXiv e-prints
Douglas, L. S., Bremer, M. N., Lehnert, M. D., Stanway, E. R., & Milvang-Jensen, B. 2010, ArXiv e-prints (D10)
Finkelstein, S. L., Papovich, C., Giavalisco, M., et al. 2009, ArXiv e-prints
Giavalisco, M. 2002, ARA&A, 40, 579
Giavalisco, M., Koratkar, A., & Calzetti, D. 1996, ApJ, 466, 831
Greiner, J., Krühler, T., Fynbo, J. P. U., et al. 2009, ApJ, 693, 1610
Hickey, S., Bunker, A., Jarvis, M. J., Chiu, K., & Bonfield, D. 2010, MNRAS, 404, 212
Hu, E. M., Cowie, L. L., Barger, A. J., et al. 2010, ArXiv e-prints
Iye, M., Ota, K., Kashikawa, N., et al. 2006, Nature, 443, 186
Labbé, I., González, V., Bouwens, R. J., et al. 2010, ApJ, 708, L26
Mannucci, F., Buttery, H., Maiolino, R., Marconi, A., & Pozzetti, L. 2007, A&A, 461, 423
McLure, R. J., Dunlop, J. S., Cirasuolo, M., et al. 2010, MNRAS, 403, 960
Oesch, P. A., Bouwens, R. J., Illingworth, G. D., et al. 2010, ApJ, 709, L16
Ota, K., Iye, M., Kashikawa, N., et al. 2010, ArXiv e-prints
Ouchi, M., Mobasher, B., Shimasaku, K., et al. 2009, ApJ, 706, 1136
Ouchi, M., Shimasaku, K., Furusawa, H., et al. 2010, ArXiv e-prints
Pentericci, L., Grazian, A., Scarlata, C., et al. 2010, A&A, 514, A64+
Reddy, N. A. & Steidel, C. C. 2009, ApJ, 692, 778
Salvaterra, R., Della Valle, M., Campana, S., et al. 2009, Nature, 461, 1258
Schaerer, D. & de Barros, S. 2010, ArXiv e-prints
Shapley, A. E., Steidel, C. C., Pettini, M., & Adelberger, K. L. 2003, ApJ, 588, 65 (S03)
Stanway, E. R., Bunker, A. J., Glazebrook, K., et al. 2007, MNRAS, 376, 727 (S07)
Stark, D. P., Ellis, R. S., Chiu, K., Ouchi, M., & Bunker, A. 2010, ArXiv e-prints
Tanvir, N. R., Fox, D. B., Levan, A. J., et al. 2009, Nature, 461, 1254
Vanzella, E., Giavalisco, M., Dickinson, M., et al. 2009, ApJ, 695, 1163 (V09)
Wilkins, S. M., Bunker, A. J., Ellis, R. S., et al. 2010a, MNRAS, 403, 938
Wilkins, S. M., Bunker, A. J., Lorenzoni, S., & Caruana, J. 2010b, ArXiv e-prints
Zheng, Z., Cen, R., Trac, H., & Miralda-Escudé, J. 2010, ApJ, 716, 574